Med Biol Eng Comput (2014) 52:283–291
DOI 10.1007/s11517-013-1065-2

ORIGINAL ARTICLE

# Modelling clavicular and scapular kinematics: from measurement to simulation

**Bart Bolsterlee · H. E. J. Veeger · F. C. T. van der Helm**

Received: 16 November 2012 / Accepted: 18 March 2013 / Published online: 30 March 2013


**Abstract** Musculoskeletal models are intended to be used to assist in prevention and treatments of musculoskeletal disorders. To capture important aspects of shoulder dysfunction, realistic simulation of clavicular and scapular movements is crucial. The range of motion of these bones is dependent on thoracic, clavicular and scapular anatomy and therefore different for each individual. Typically, patient or subject measurements will therefore not fit on a model that uses a cadaveric morphology. Up till now, this problem was solved by adjusting measured bone rotations such that they fit on the model, but this leads to adjustments of on average 3.98° and, in some cases, even more than 8°. Two novel methods are presented that decrease this discrepancy between experimental data and simulations. For one method, the model is scaled to fit the subject, leading to a 34 % better fit compared to the existing method. In the other method, the set of possible joint rotations is increased by allowing some variation on motion constraints, resulting in a 42 % better fit. This change in kinematics also affected the kinetics: muscle forces of some important scapular stabilizing muscles, as predicted by the Delft Shoulder and Elbow Model, were altered by maximally 17 %. The effect on the glenohumeral joint contact force was however marginal (1.3 %). The methods presented in this paper might lead to more realistic shoulder simulations and can therefore be considered a step towards (clinical) application, especially for applications that involve scapular imbalance.

**Keywords** Musculoskeletal model · Shoulder kinematics · Scapulothoracic · Subject specific

**Electronic supplementary material** The online version of this article (doi:10.1007/s11517-013-1065-2) contains supplementary material, which is available to authorized users.

B. Bolsterlee (✉) · H. E. J. Veeger · F. C. T. van der Helm
Biomechatronics & Bio-robotics group, Dept. of Biomechanical Engineering, Delft University of Technology, Delft, The Netherlands
e-mail: b.bolsterlee@tudelft.nl

H. E. J. Veeger
Faculty of Human Movement Science, Research Institute MOVE, VU University Amsterdam, Amsterdam, The Netherlands

## 1 Introduction

Musculoskeletal models of the human shoulder are intended to be used for a variety of purposes, for instance, to predict surgical outcome, to improve diagnosis of musculoskeletal diseases or to provide insight into human function. For simulations with a large-scale musculoskeletal model with multiple segments, several degrees of freedom (DOF) and many muscle elements, the most commonly used method is an inverse dynamic analysis. Measured kinematics and external forces serve as input to the model and are used to calculate the associated net joint moments around joints. If muscle functions, usually muscle forces or activations, are also desired as an output, the muscle redundancy problem can be solved by selecting a set of muscle forces that can produce these joint moments while minimising an objective criterion like muscle stress or muscle energy expenditure [24].

Because the most detailed models require anatomical parameters that, at least up till now, cannot be measured in vivo, data obtained from cadaver studies are commonly used [19]. For model estimations based on motion recordings, the most straightforward method is to impose the in vivo measured bone orientations as such to the model. For a system where joint rotations are not coupled ("open-loop" systems like for example the hip, knee and

elbow joints), this is a feasible method, but for closed kinematic chains like the shoulder, this method will be problematic since, dependent on the differences in dimensions between model and subject, not all combinations of joint rotations as measured in vivo will be reproducible for the model. For the shoulder girdle, the closed chain is formed by combined motion of clavicle and scapula [articulating at the acromioclavicular (AC) joint] to the thorax. This motion is restricted on the anterior side by the sternoclavicular (SC) joint and on the posterior side by the scapulothoracic gliding plane that constrains the medial border of the scapula to remain in contact with the thoracic wall. Another important limitation in relative motion of the bones of the shoulder girdle is formed by the coracoclavicular ligaments, which constrain movements between clavicle and scapula and especially play an important role in the axial rotation of the clavicle [25]. Combinations of SC- and AC-joint rotations are therefore limited and of course dependent on the shape of thorax, clavicle and scapula, as well as on location of SC- and AC-joint rotation centres.

For musculoskeletal shoulder models, this means that as a result of differences in dimension between subject and model, movements as measured on a subject can often not be reproduced by the model. Neglecting the interaction between clavicle, scapula and thorax or using regression equations for the input of scapular and clavicular angles [8] as is the case in some upper extremity models [9, 16], would however limit its clinical use, because key aspects of shoulder dysfunction can only be captured by modelling the (abnormal) behaviour of the full chain of segments that provide the stability and mobility of the shoulder [31].

In this study, an existing method to realistically simulate measured shoulder kinematics will be compared to two variations to this method.

In the existing method, measured kinematics are adjusted to fit the model. In [7], a *kinematic optimisation* was proposed which calculates simulated rotations of scapula and clavicle by mathematical minimisation of the difference between measured and simulated bone angles, while satisfying two *motion constraints* that model the scapulothoracic gliding plane (1 and 2) and one motion constraint that defines the behaviour of the coracoclavicular ligament. In the original setting, this behaviour was constrained as a constant length of the conoid ligament only (3). Motion constraints were defined as:

1. The distance from the trigonum spinae (TS) of the scapula to the thorax is constant.
2. The distance from the angulus inferior (AI) of the scapula to the thorax is constant.
3. The conoid ligament has a constant length.

The method described above has been implemented in the most recently published version of the Delft Shoulder and Elbow Model (DSEM) [23, 29] and was later also applied in the UK National Shoulder Model [5]. Other comprehensive shoulder models [2, 4, 10, 12, 14, 15, 18, 26] also model the scapulothoracic gliding plane as a constant distance from two points on the scapula to the thorax, but they do not describe how they assure that measured angles, or those derived from regression equations, satisfy these constraints. This kinematic optimisation aims to find the best compromise between staying close to experimental data, while obtaining an anatomically realistic simulation. However, when morphological differences between subject and model are large, differences between measured and simulated orientations also increase and it can be questioned whether the simulation still resembles the measurements. For the five subjects that De Groot [7] analysed, average differences over 10° for some angles (scapular tilt and clavicular protraction) resulted. It can also be argued that the assumptions that the medial border of the scapula is always on the same distance to the thorax and the conoid ligament is of constant length are not realistic for all shoulder positions, and at least that these values are not identical for each individual. It is not known what effect these assumptions have on model predictions.

In this study, two variations to the kinematic optimisation as proposed by De Groot et al. [7] will be presented: firstly, the constraints that define the distance between scapula and thorax will be set to soft constraints, allowing for some variation in distance between medial border and thorax and conoid length. Secondly, the opposite approach to changing measurements to fit the model will be evaluated, namely changing the model to fit the subject, loosely described as ‘scaling’. We expect that the model adaptation (soft constraint) and model scaling will result in a closer fit between simulated and recorded angles for subjects of different build. We also expect that using soft constraints will significantly influence the resulting kinetics.

## 2 Methods

### 2.1 Kinematic optimisation

Orientations of clavicle and scapula with respect to the thorax were expressed as the six Euler angles proposed by the ISB [33]: protraction, elevation and axial rotation of the clavicle and protraction, lateral rotation, and anterior tilt of the scapula. From these measured angles ($\bar{\theta}_{\text{meas}}$), simulated angles ($\bar{\theta}_{\text{sim}}$) were obtained by minimisation of the weighted sum of $J_\theta$ and $J_{\text{con}}$:

$$\min_{\bar{\theta}_{\text{sim}}}(J_\theta + \text{wf} \cdot J_{\text{con}}) \quad (1)$$

with $J_\theta$ the summed squared difference between $\bar{\theta}_{\text{meas}}$ and $\bar{\theta}_{\text{sim}}$

$$J_\theta = \sum_{i=1}^{6} \left(\bar{\theta}_{\text{sim}}(i) - \bar{\theta}_{\text{meas}}(i)\right)^2 \quad (2)$$

where $i$ represents the number of the orientation angle, and $J_{\text{con}}$ the squared deviation from three motion constraints (which are dependent on the morphology that is used by the model)

$$J_{\text{con}} = (\text{dTS}_{\text{sim}} - \text{dTS}_0)^2 + (\text{dAI}_{\text{sim}} - \text{dAI}_0)^2 + \left(\ell_{\text{con,sim}} - \ell_{\text{con},0}\right)^2 \quad (3)$$

with $\text{dTS}_{\text{sim}} = \|\text{TS} - \text{ellipsoid}\|$ and $\text{dAI}_{\text{sim}} = \|\text{AI} - \text{ellipsoid}\|$ the simulated Euclidean distance from landmarks TS and AI to the projection of these points on the ellipsoidal surface that describes the thoracic wall and $\ell_{\text{con,sim}}$ the simulated conoid length (defined as the Euclidean distance from conoid origin on the clavicle to insertion on the scapula). $\text{dTS}_0$, $\text{dAI}_0$ and $\ell_{\text{con},0}$ are the three reference values for the three motion constraints and have values of, respectively, 3.71, 2.67 and 1.94 cm in the generic model (see next section and Online resource 1). Deviations from these reference values will lead to a higher value of $J_{\text{con}}$. The weight factor wf weighs the relative contribution of satisfying motion constraints ($J_{\text{con}}$) and staying close to experimental data ($J_\theta$). $\text{wf} = 0$ means that any deviation from motion constraints remains unpunished, resulting in an exact match of simulated and measured angles but possibly large deviations from motion constraints (e.g. unrealistic large distance from the scapular medial border to the thoracic wall). With $\text{wf} = \infty$, the results are similar to the kinematic optimisation proposed by De Groot et al. [7], where measured positions are adjusted to simulated positions such that they exactly match the reference values for motion constraints.

## 2.2 Experimental data

Three male and two female subjects, selected on the basis of large inter-individual differences (age 29.2 ± 2.3 year, body length 176.3 ± 7.2 cm) participated in this study. Informed consent was obtained from all subjects. The study adhered to the ethical guidelines of the 1975 Declaration of Helsinki.

Locations of bony landmarks as described by Wu et al. [33] and one additional landmark, namely the most laterally palpable part of the thorax (ThL) were digitised in the anatomical posture. 3D kinematics during two shoulder movements, abduction (ABD) and anteflexion (FLEX), were recorded. An Optotrak system (Northern Digital, Inc., Waterloo, Ontario, Canada) with four units was used to collect marker positions (sampled at 100 Hz) of four clusters of (skin-fixed) markers on thorax, humerus and forearm of the subject and to a scapula locator [28], which was manually positioned on three bony landmarks of the scapula during the recorded movements. Marker data were transformed to segment coordinate systems and Euler angles calculated according to ISB convention [33]. Because no marker cluster can be placed on the clavicle without significant influence of skin motion and only two landmarks can be palpated (SC and AC), clavicular protraction and elevation were derived by assuming that the palpable landmarks SC and AC were rigidly connected to thorax and scapula, respectively. Axial rotation was calculated by a method that assumes minimal rotation in the AC joint [30]. Angles were sampled at steps of 5° of humeral elevation from 30° to 120°, leading to one set of $\bar{\theta}_{\text{meas}}$ per subject, motion and step of elevation.

## 2.3 Generic and subject-specific morphological parameters

The generic version of the model used in this study was based on a morphological parameter set that was measured on the cadaver of a 57-year-old male [19]. Relevant parameters for kinematic optimisation are: the midpoint and axes of the ellipsoid that describe the thorax, the coordinates of landmarks of the scapula, clavicle and thorax in the anatomical position, the SC- and AC-joint rotation centres and the origin and insertion of the conoid ligament (Online resource 1). The ellipsoid centre was assumed to be in the midpoint of PX-T8, the axes (constrained to be coincident with the axes of the thorax coordinate system) were calculated by minimisation of the squared distance from 259 points that were palpated on rib 1 to 9 to the projection of these points on the ellipsoidal surface. The model that uses this parameter set will be referred to as the generic model or GM.

A subject-specific model (SM) was created from landmark positions of thorax, clavicle and scapula as palpated on the subject. The ellipsoid axes were scaled in the $z$-direction (thorax width) by the ratio between $z$-coordinate of landmark ThL of subject and cadaver, in the $y$-direction (thorax height) by ratio between the distance from midpoint of landmark IJ-C7 to the midpoint of PX-T8 and in the $x$-direction (thorax depth) by the ratio between the distance from midpoint IJ–PX to midpoint C7–T8. The midpoint of C7–T8 was used as ellipsoid centre (as in GM). The coordinates of the origin of the conoid ligament were scaled linearly by the ratio of clavicle lengths, defined as distance from SC to AC. The scapular insertion of the conoid ligament was transformed from the generic dataset to the subject by a linear transformation method proposed

in [20]. SC- and AC-joint centres were assumed to have an equal offset to palpable landmarks SC and AC as for the generic parameter set. Reference values $dTS_0$ and $dAI_0$ for the motion constraints were made subject specific by calculating the distance of palpated TS and AI to the scaled thoracic ellipsoid in the anatomical position. The reference conoid length was assumed to be 1.94 cm for both the model and all subjects [13]. See Online resource 1 for all coordinates of morphological parameters.

### 2.4 Model simulations

For each subject, motion and step of humeral elevation $\bar{\theta}_{sim}$, $\ell_{con,sim}$, $dTS_{sim}$ and $dAI_{sim}$ were calculated by minimising Eq. (1) with a FORTRAN-based optimisation program [34] for two model versions—the generic model (GM) and the subject-specific model (SM)—and for three values of wf, namely one where motion constraints are not weighed at all (wf = 0, no constraints or NoC), one where motion constraints almost exactly match their reference values (wf = 5, hard constraints or HaC) and one value which, as we will later show, results in a satisfactory compromise between matching motion constraints and staying close to measured angles (wf = 0.01, soft constraints or SoC).

To ensure that the optimisation finds the global minimum, each optimisation was repeated ten times with ten different initial guesses, randomly varied with maximally 7.5° around $\bar{\theta}_{meas}$. The result with the lowest value of the objective function was used.

The DSEM [23] was used to calculate net joint moments, muscle moment arms, muscle forces and joint reaction forces for simulations with GM and all three values of wf. Minimal energy expenditure was used as load sharing criterion [24]. Since there is no general rule for scaling of muscle activation parameters while kinetic model predictions are extremely sensitive to variations in these [1], we decided to limit our kinetic analysis of the effects of kinematic optimisation to GM simulations only.

To further evaluate the influence of the weight factor, the kinematic optimisation was also run for 25 values between 0.0001 and 0.04 for motion ABD.

### 2.5 Comparison

For each condition, subject, motion and step of humeral elevation, the *root mean square difference* ($RMSD_\theta$) between $\bar{\theta}_{meas}$ and $\bar{\theta}_{sim}$ was calculated:

$$RMSD_\theta = \sqrt{\frac{1}{6}\sum_{i=1}^{6}\left(\bar{\theta}_{sim}(i) - \bar{\theta}_{meas}(i)\right)^2} \quad (4)$$

with $i$ the angle number.

A low $RMSD_\theta$ value indicates a small discrepancy between measurement and simulation. The influence of constraints (HaC vs. SoC), model version (GM vs. SM) and motion (FLEX and ABD) on the $RMSD_\theta$ was evaluated using a repeated measures ANOVA (between subjects measures: *constraints*, *model version*, *motion* and *elevation*). Normality was verified using the Shapiro–Wilk test. A significance level of $\alpha = 0.05$ was maintained.

## 3 Results

Without constraints (NoC), measured angles were exactly matched by the model, but the distance from TS to the thorax ($dTS_{sim}$) was, in some cases, more than 7 cm (>4 cm deviation from its reference value) which we consider to be large for healthy movements (Fig. 1). In some cases, NoC simulations resulted in a scapula that was positioned inside the ribcage, which of course is not realistic. Deviations from motion constraints were on average 1.83, 1.26 and 0.42 cm for, respectively, distance from TS and AI to the thorax and conoid length (Fig. 3). Maximum deviation was 4.36 cm (distance from TS to the thorax). Motion constraints were almost exactly satisfied with hard constraints (HaC), but simulated rotations differed on average 3.29° ± 0.75° from experimentally obtained values (Table 1), with a maximum difference exceeding 8° (Fig. 2).

With soft constraints (SoC), values for motion constraints were kept closer to reference values (e.g. $|dTS_{sim} - dTS_0| < 1$ cm) than NoC, and simulated rotations were staying closer to measurements (1.90° ± 0.53°, 42 % improvement) than HaC simulations. There was a significant main effect of type of constraint on $RMSD_\theta$ ($F_{1,4} = 369.42$, $p = 0.001$). This was expected as the weight factor wf changes the way the optimisation penalises the difference between the measured and simulated angles.

Subject-specific modelling also improved the fit of experimental data on model simulations: the mean $RMSD_\theta$ decreased from 3.14° ± 0.99° for GM to 2.05° ± 0.62° for SM (Table 1). This effect did not reach significance ($F_{1,4} = 226.23$, $p = 0.086$) but a trend was visible ($p < 0.1$) where the $RMSD_\theta$ values were on average 34 % smaller for SM than GM. The use of a subject-specific model with soft constraints was accompanied by a decrease in deviations from motion constraints for distance from TS to the thorax and conoid length. Deviations in distance from AI to the thorax were slightly larger (Fig. 3).

The combination of SoC and SM resulted in an average $RMSD_\theta$ of 1.50°, 62 % lower than the existing method (GM + HaC, Fig. 2). Distance from TS and AI to the

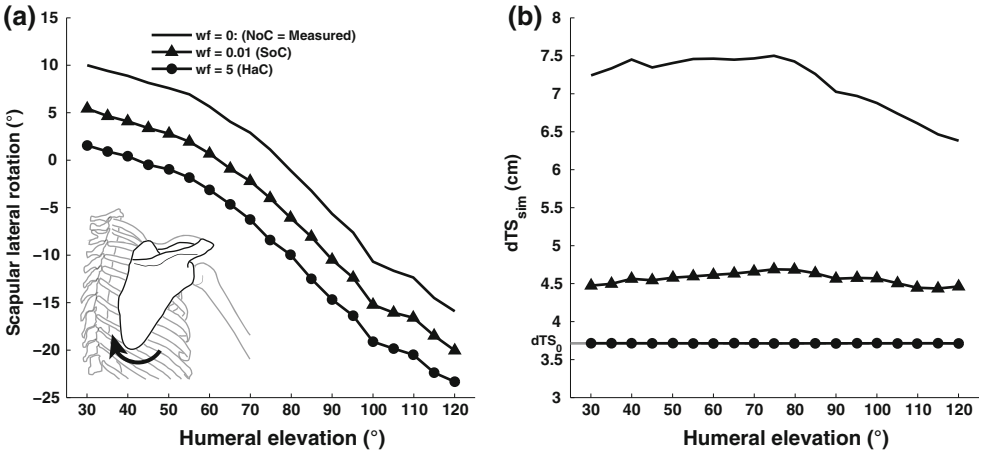


**Fig. 1** Effect of soft constraints: typical example of how measurements are changed for realistic simulation of FLEX with the generic model for one subject calculated without constraints (NoC, *line*), soft constraints (SoC, *triangles*) and hard constraints (HaC, *circles*) for (**a**) one of the six optimised angles: scapular lateral rotation; (**b**) deviation from one of the motion constraints ($dTS_{sim}$, simulated distance from TS to the thorax)

**Table 1** The effects of type of constraints, model type and motion on RMSD, including significance values

| | $RMSD_\theta$ | $p$ value |
|---|---|---|
| Constraints | | |
| HaC | 3.29 ± 0.75 | 0.001* |
| SoC | 1.90 ± 0.53 | |
| Model version | | |
| GM | 3.14 ± 0.99 | 0.086 |
| SM | 2.05 ± 0.62 | |
| Motion | | |
| ABD | 2.26 ± 1.17 | 0.169 |
| FLEX | 2.92 ± 1.67 | |

* Indicates statistical significance at $p < 0.05$

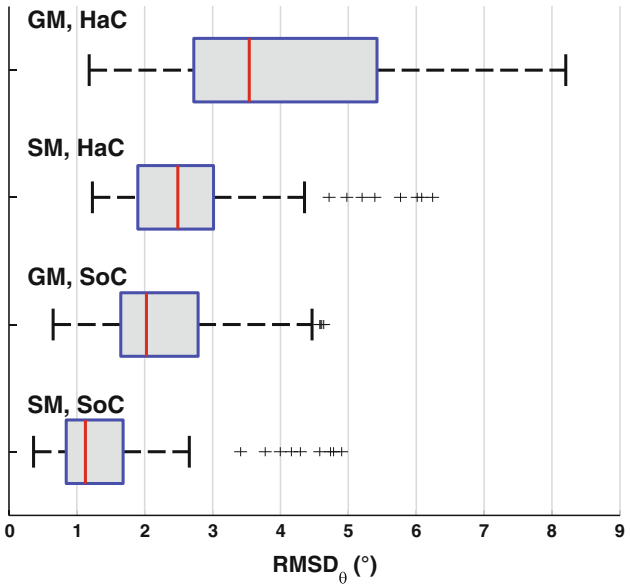


**Fig. 2** Boxplot of RMSD per method for both model version (GM and SM) and two constraint types (HaC and SoC). The model without constraints is not plotted, since the RMSD is always zero for that condition

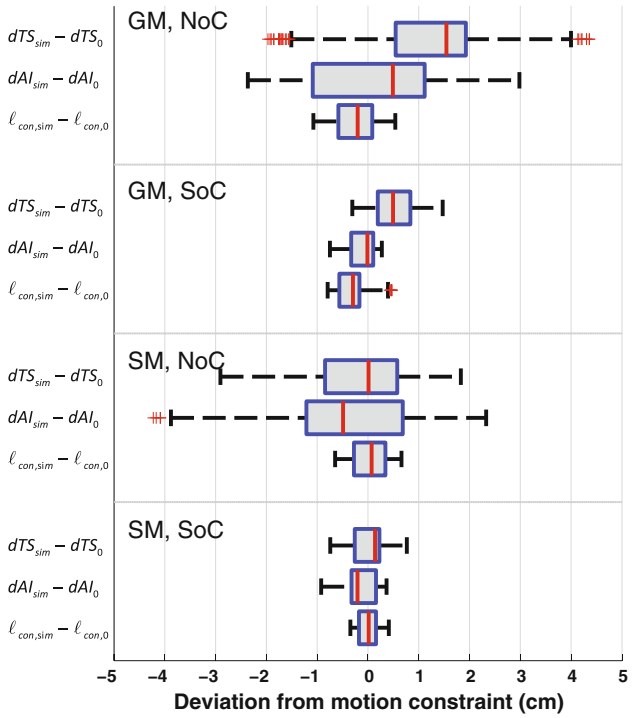


**Fig. 3** Boxplot of the deviations from the three motion constraints for four conditions: without constraints (NoC), soft constraints (SoC), generic (GM) and subject specific (SM). The model with hard constraints is not shown, because deviations from motion constraints are always zero for that condition

thorax was on average 0.28 ± 0.16 and 0.27 ± 0.16 for this condition.

There was no significant main effect on motion ($F_{1,4} = 8{,}019$, $p = 0.169$) and no interaction effects reached significance.

Figure 4 shows the effect of weight factor on resemblance between measured and simulated angles on the one hand (RMSD), and deviation from motion constraints on the other for an abduction movement with the generic

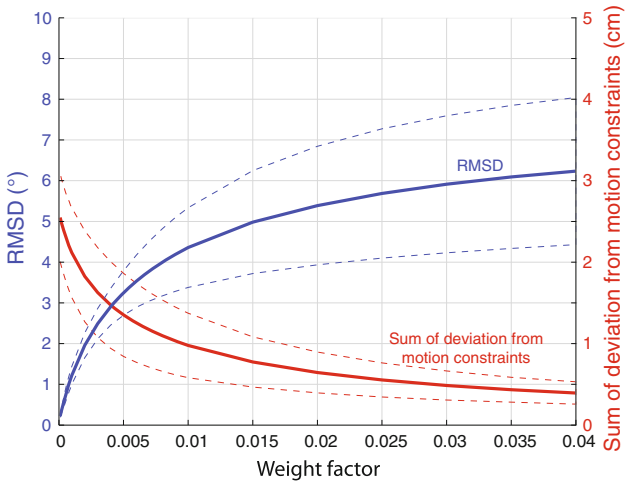


**Fig. 4** Effect of weight factor on RMSD values and sum of absolute deviation from motion constraints (motion: ABD, model: GM). *Solid lines* represent the mean values over all five subjects, *thin lines* are the standard deviations

model. At wf = 0.01, the total deviation from motion constraints was on average 2 cm.

In the generic model, clavicular elevation (−2.59° ± 3.12° for ABD and −4.33° ± 4.82° for FLEX) and scapular lateral rotation (3.03° ± 3.43° for ABD and 4.50° ± 5.18° for FLEX) were changed the most (Table 2). To fit the measurements on the subject-specific model, anterior tilt of the scapula was adjusted most (1.95° ± 3.58° for ABD and 2.17° ± 3.72° for FLEX).

DSEM-predicted muscle forces for two important scapular stabilising muscles (trapezius, serratus anterior) and glenohumeral joint contact force (GH-JCF) during FLEX are shown in Fig. 5. Averaged over all 19 steps of humeral elevation and all five subjects, the serratus anterior was 3.0 % (maximum 6.4 %) more active with SoC than with HaC. The force of the trapezius muscle was almost equal for both conditions, but with SoC, the clavicular part produced 17 % (5.2 N) less force while the scapular part was predicted to be 6.8 % (6.0 N) more active. The rhomboid (not shown) was predicted to be inactive for both FLEX and ABD and for all conditions. The difference in kinematics between hard and soft constraints had only a small effect on the GH-JCF. With SoC, the GH-JCF was on average 1.30 % (5.7 *N*) higher than with HaC, with a maximum difference of 2.97 % (13 *N*) .

## 4 Discussion

In some cases, the direct use of measured angles for model simulations resulted in scapula positions in which the medial border of the scapula fell inside or was very far off the thorax (>7 cm, Fig. 1), which confirms the assumption by Van der Helm [29] and De Groot [7] that motions of the scapula with respect to the thoracic wall should be restricted. However, from the on average almost 4° difference between measured and simulated kinematics when using the existing method (HaC + GM) that restricts clavicular and scapular motions to exactly satisfy motion constraints, we conclude that a fixed length constraint might be too rigid. Therefore, we proposed a method that allows some variation in motion constraints. This method, called 'soft constraints', resulted in a closer match of simulated kinematics on experimental recordings (42 %) compared to hard constraints. Motion constraints were also kept closer to reference values than without constraints (on average 65 % less deviation than with HaC, Fig. 3). Instead of adapting measurements to fit the model, the

**Table 2** Measured clavicular (clav.) and scapular (scap.) angles (averaged over all steps of humeral elevation and subjects) and the difference with simulated kinematics per model version, constraint type and two movements [abduction (ABD), anteflexion (FLEX)]

| Motion | Angle | Measured (°) | Difference between simulated and measured (°) | | | |
|---|---|---|---|---|---|---|
| | | | GM, HaC | SM, HaC | GM, SoC | SM, SoC |
| ABD | Clav. protraction | −29.52 ± 7.44 | −1.57 ± 2.03 | 1.04 ± 2.69 | −1.02 ± 1.67 | 1.03 ± 2.00 |
| | Clav. depression | −15.12 ± 5.37 | −2.59 ± 3.12 | 0.49 ± 2.00 | −1.20 ± 1.40 | 0.13 ± 0.96 |
| | Clav. axial rotation | 13.44 ± 8.47 | 0.77 ± 1.51 | −0.62 ± 0.80 | 0.28 ± 0.37 | −0.06 ± 0.21 |
| | Scap. protraction | 26.20 ± 4.06 | 1.71 ± 2.05 | −0.99 ± 3.09 | 1.16 ± 1.72 | −1.05 ± 2.48 |
| | Scap. medial rotation | −17.25 ± 10.74 | 3.03 ± 3.43 | −1.62 ± 1.65 | 1.58 ± 1.53 | −0.72 ± 0.82 |
| | Scap. anterior tilt | −1.80 ± 4.09 | 1.57 ± 3.56 | 1.95 ± 3.58 | 0.78 ± 1.85 | 0.87 ± 2.49 |
| FLEX | Clav. protraction | −17.09 ± 5.16 | −2.57 ± 3.06 | −0.33 ± 1.87 | −1.86 ± 3.02 | 0.01 ± 1.58 |
| | Clav. depression | −14.24 ± 8.81 | −4.33 ± 4.82 | −0.76 ± 2.45 | −1.95 ± 2.00 | −0.36 ± 0.90 |
| | Clav. axial rotation | 9.82 ± 7.11 | 1.26 ± 2.31 | −0.38 ± 1.38 | 0.39 ± 0.51 | 0.01 ± 0.26 |
| | Scap. protraction | 38.32 ± 8.06 | 3.31 ± 3.58 | 1.29 ± 2.99 | 2.26 ± 3.32 | 0.26 ± 2.12 |
| | Scap. medial rotation | −10.68 ± 8.48 | 4.50 ± 5.18 | 0.32 ± 2.23 | 2.67 ± 2.52 | 0.40 ± 0.95 |
| | Scap. anterior tilt | −3.56 ± 4.46 | 1.49 ± 4.30 | 2.17 ± 3.72 | 0.59 ± 2.23 | 0.70 ± 2.21 |

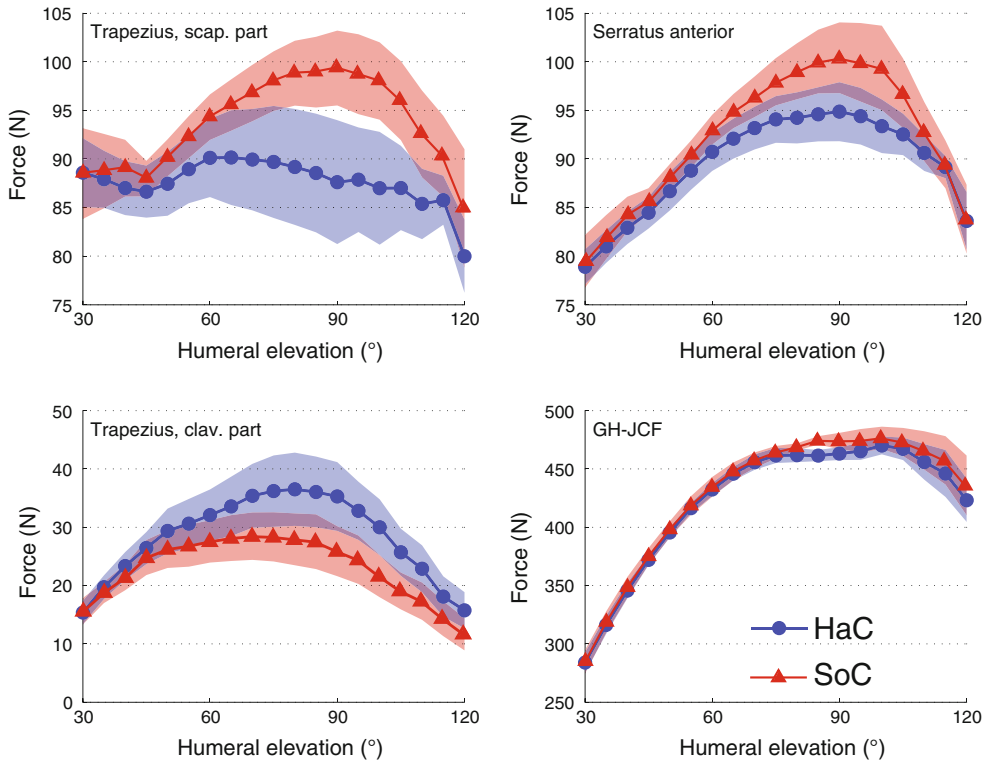


**Fig. 5** Generic model force predictions for FLEX for two important scapular stabilizing muscles while using hard constraints (HaC, *blue circles*) and soft constraints (SoC, *red triangles*): the trapezius (both the part that attaches to the clavicle and the part that attaches to the scapula) and the serratus anterior. The glenohumeral joint contact force (GH-JCF) is also shown. All data are averaged over all five subjects and the *shaded areas* represent standard error of the mean (colour figure online)

opposite approach was also tested, namely scaling the model to fit the subject (SM). This resulted in a 34 % lower $RMSD_\theta$ compared to the original model. A combination of both adaptations (SM + SoC) decreased $RMSD_\theta$ the most, by 62 %. This was accompanied by only a small deviation from motion constraints (0.24 cm on average). Both scaling and using soft constraints resulted in an improvement of the match of recordings on simulated shoulder kinematics and can therefore be considered an improvement to the existing method.

The soft constraint method proposed in this study aims to find a balance between matching motion constraints and staying close to recorded bone rotations. By choosing a low value of wf, much variation is allowed on motion constraints, resulting in a low $RMSD_\theta$. We chose to use a value of $wf = 0.01$ to evaluate the effect of soft constraints, because this was the value for which the sum of the three motion constraints deviated on average 2 cm (Fig. 4). We consider this deviation realistic, as we will explain in the next paragraph. We however do not claim this value to be the optimal value, since we could not quantitatively verify the effect of the weight factor on model predictions of muscle forces.

Some freedom in the distance between the medial border of the scapula and the thorax is justified for two reasons. First, some variation is expected in reality, because this distance is the result of a force balance between the muscles that attach to thorax and scapula (mainly the serratus anterior, trapezius and the rhomboid), the reaction force of the thorax and the force the skin exerts on the scapula and therefore dependent on muscle activations. Secondly, this distance cannot be determined very accurately. The error associated with the simplified representation of the ribcage by an ellipsoid is 5.9 mm (the root mean square distance from all 259 points that were palpated on the ribs of the cadaver to the surface of the least-squares best-fit ellipsoid). This means that the model calculated distance to the thoracic ellipsoid is on average 5.9 mm different from the actual distance. For these two reasons, deviations from motion constraints in the order of 2–6 mm with a maximum of 14.7 mm, when soft constraints were used, are considered to be realistic and the use of soft constraints is therefore recommended. Furthermore, the use of soft constraints also allows for analysis of scapular pathologies such as scapular winging. This abnormality can be caused by palsy of scapular stabilising muscles (trapezius, serratus anterior, rhomboid), leading to an increased mobility of the scapula, which cannot be modelled by constraining the scapula to be on a fixed distance to the thorax. In absence or with severely decreased active scapular stabilisation,

passive tissues such as the skin are expected to limit scapular movements, so this should also be incorporated when attempting to model scapular winging.

The improved match of simulations on measurements by 34 % with the scaled model is in line with the prevailing opinion that subject-specific models give more accurate model results. However, for the individualised model, only the effect of scaling on the kinematic level was studied. Kinetic model results were only calculated with the DSEM for GM, because it is not known how soft tissue properties such as force–length–velocity characteristics and muscle attachments scale with bone geometry [32]. For the lower limb, it has been shown that inter-individual differences can often not be captured by scaling from a generic model [11]. In the present study, a relatively simple and very accessible method to individualise the model's bone geometry was adopted, namely scaling from palpated landmarks. With the recent advancements in medical imaging techniques such as ultrasound, MRI and CT, more information of anatomical structures become available, enabling development of more detailed subject-specific models. It is expected that higher detail further improves the fit of model simulations on measurements. However, even though these models might lead to more accurate estimations of some model variables such as muscle moment arms and musculotendon lengths [3, 27], improvements to more clinically relevant model outputs such as muscle forces and joint contact forces remain unclear, because quantitative validation of these outputs is very difficult and only based on patient data [22]. Based on sensitivity analyses, it can even be expected that exactly those parameters which are most difficult to individualise (tendon lengths, force–length curves) influence model predictions the most [1]. The current challenge of subject-specific modelling is to prove whether new assumptions that are necessarily introduced when individualising a model are more valid than the assumptions of a generic model, namely that the subject's morphology resembles the model.

The glenohumeral contact force was only marginally affected by the type of constraint (1.3 % difference). For FLEX, some increased activity of the serratus anterior and a shift of force production from the clavicular part to the scapular part of the trapezius muscle were predicted by the DSEM when using soft constraints compared to the original model with hard constraints (Fig. 5). Activation of these muscles during abduction and anteflexion is in accordance with findings of an EMG study [21]. Inactivity of the rhomboid during FLEX and ABD as predicted by the DSEM is not in agreement with this study. Since there is no quantitative validation possible of musculoskeletal models on the level of individual muscle forces, it can only be concluded that the type of constraint does influence the model predictions, but it cannot be said which method is more realistic. A comparison of EMG recordings with predicted muscle forces could theoretically be used for further quantitative evaluation. However, this would require an accurate method to calculate muscle forces from EMG recordings under dynamic conditions, which is not yet available.

From the relatively large bands of inter-subject variation (shaded areas in Fig. 5), it can be concluded that incorporating the individualised motion pattern of clavicular and scapular movements (significantly) influences model outcome. Using regression equations to describe these motions therefore strongly limits the potential of a model to differentiate between subjects. The model that was dubbed 'generic' in the present study could therefore also be called subject specific, since the individualised input leads to model outcome that is dependent on the subject. A model with individualised soft tissue parameters can be expected to enlarge the variation in kinetic predictions between subjects, but since quantitative validation is not (yet) possible, it cannot be concluded whether this would be an improvement.

Errors of tracking clavicle and scapula of course also propagate to simulated kinematics. The scapula was tracked with the most reliable motion-capture method available, the scapula locator. The error of palpation of landmarks is estimated to lead to approximately 2° error on bone rotation angles [6]. This value almost equals the $RMSD_{\theta}$ for the subject-specific model and the model with soft constraints. It is therefore possible that rotations after kinematic optimisation are closer to the actual ones than the ones measured.

Only clavicular and scapular orientations that were measured between 30° and 120° of humeral elevation were used for this study. During the motion recordings, it was found that tracking the scapula with the scapula locator was not always reliable for higher humeral elevation angles, as for some subjects one of the scapular landmarks, the angulus acromialis, was difficult to palpate because of substantial soft tissue covering by the (activated) medial and posterior parts of the deltoid muscle. So in addition to the earlier reported inaccuracies of skin-mounted marker clusters [17, 28], in this study, it was observed that also the scapula locator has less fidelity for tracking the scapula at higher humeral elevation levels and therefore remains problematic. More reliable (but also much less accessible) techniques such as dynamic CT, dynamic MRI or (stereo) fluoroscopy measurements might in the future provide more detailed information on shoulder kinematics. These techniques could also be used to check whether kinematic optimisation leads to simulated movements that are closer to the actual ones and thus compensate for measurement errors. This could also lead to recommendations on what angles can be weighed more heavily in the optimisation, because they can more reliably be tracked.

In summary, two adaptations to an already existing method have been proposed that reduce the discrepancy

between simulated and measured clavicular and scapular kinematics in a musculoskeletal shoulder model. One method does so by relaxing the constraints on movements of these bones within physiological boundaries (42 % lower difference between measurement and simulation), the other by scaling the morphology of the model to the subject (34 % improvement). As long as there is no 'gold standard' for quantitative evaluation of kinetic model predictions, musculoskeletal model adaptations can only be evaluated based on differences between versions or rather inaccurate measures such as EMG. Therefore, we were unfortunately not able to verify whether the kinetic predictions are indeed more realistic, as we would expect them to be, based on the improved kinematical fit.

**Acknowledgments** The research leading to these results has received funding from the European Information and Communication Technologies Community Seventh Framework Program (FP7/2007-2013) under grant agreement no. 248693.

## References

1. Ackland DC, Lin Y-C, Pandy MG (2012) Sensitivity of model predictions of muscle function to changes in moment arms and muscle–tendon properties: a Monte-Carlo analysis. J Biomech 45(8):1463–1471
2. Ambrósio J, Quental C, Pilarczyk B et al (2011) Multibody biomechanical models of the upper limb. Symposium on human body dynamics, pp 4–17
3. Arnold AS, Salinas S, Asakawa DJ et al (2000) Accuracy of muscle moment arms estimated from MRI-based musculoskeletal models of the lower extremity. Comput Aided Surg 5(2):108–119
4. Blana D, Hincapie JG, Chadwick EK et al (2008) A musculoskeletal model of the upper extremity for use in the development of neuroprosthetic systems. J Biomech 41(8):1714–1721
5. Charlton IW, Johnson GR (2006) A model for the prediction of the forces at the glenohumeral joint. Proc Inst Mech Eng, Part H: J Eng Med 220(8):801–812
6. de Groot JH (1997) The variability of shoulder motions recorded by means of palpation. Clin Biomech 12(7–8):461–472
7. De Groot JH (1998) The shoulder: a kinematic and dynamic analysis of motion and loading. PhD thesis, Delft University of Technology
8. de Groot JH, Brand R (2001) A three-dimensional regression model of the shoulder rhythm. Clin Biomech 16(9):735–743
9. Dickerson CR, Chaffin DB, Hughes RE (2007) A mathematical musculoskeletal shoulder model for proactive ergonomic analysis. Comput Methods in Biomech Biomed Eng 10(6):389–400
10. Dubowsky SR, Rasmussen J, Sisto SA et al (2008) Validation of a musculoskeletal model of wheelchair propulsion and its application to minimizing shoulder joint forces. J Biomech 41(14): 2981–2988
11. Duda GN, Brand D, Freitag S et al (1996) Variability of femoral muscle attachments. J Biomech 29(9):1185–1190
12. Garner BA, Pandy MG (2001) Musculoskeletal model of the upper limb based on the visible human male dataset. Comput Methods Biomech Biomed Eng 4(2):93–126
13. Harris RI, Vu DH, Sonnabend DH et al (2001) Anatomic variance of the coracoclavicular ligaments. J Shoulder Elbow Surg 10(6): 585–588
14. Högfors C, Sigholm G, Herberts P (1987) Biomechanical model of the human shoulder—I. Elements. J Biomech 20(2):157–166
15. Högfors C, Peterson B, Sigholm G et al (1991) Biomechanical model of the human shoulder joint—II. The shoulder rhythm. J Biomech 24(8):699–709
16. Holzbaur KRS, Murray WM, Delp SL (2005) A model of the upper extremity for simulating musculoskeletal surgery and analyzing neuromuscular control. Ann Biomed Eng 33(6): 829–840
17. Karduna AR, McClure PW, Michener LA et al (2001) Dynamic measurements of three-dimensional scapular kinematics: a validation study. J Biomech Eng 123(2):184–190
18. Karlsson D, Peterson B (1992) Towards a model for force predictions in the human shoulder. J Biomech 25(2):189–199
19. Klein Breteler MD, Spoor CW, Van der Helm FCT (1999) Measuring muscle and joint geometry parameters of a shoulder for modeling purposes. J Biomech 32(11):1191–1197
20. Matias R, Andrade C, Veloso AP (2009) A transformation method to estimate muscle attachments based on three bony landmarks. J Biomech 42(3):331–335
21. Moseley JB, Jobe FW, Pink M et al (1992) Emg analysis of the scapular muscles during a shoulder rehabilitation program. Am J Sports Med 20(2):128–134
22. Nikooyan AA, Veeger HEJ, Westerhoff P et al (2010) Validation of the Delft Shoulder and Elbow Model using in vivo glenohumeral joint contact forces. J Biomech 43(15):3007–3014
23. Nikooyan AA, Veeger HE, Chadwick EK et al (2011) Development of a comprehensive musculoskeletal model of the shoulder and elbow. Med Biol Eng Comput 49(12):1425–1435
24. Praagman M, Chadwick EKJ, van der Helm FCT et al (2006) The relationship between two different mechanical cost functions and muscle oxygen consumption. J Biomech 39(4):758–765
25. Pronk GM, van der Helm FCT, Rozendaal LA (1993) Interaction between the joints in the shoulder mechanism: the function of the costoclavicular, conoid and trapezoid ligaments. Proc Inst Mech Eng [H] 207(4):219–229
26. Quental C, Folgado J, Ambrósio J et al (2012) A multibody biomechanical model of the upper limb including the shoulder girdle. Multibody Syst Dyn 28(1–2):83–108
27. Scheys L, Spaepen A, Suetens P et al (2008) Calculated moment-arm and muscle-tendon lengths during gait differ substantially using MR based versus rescaled generic lower-limb musculoskeletal models. Gait Posture 28(4):640–648
28. van Andel C, van Hutten K, Eversdijk M et al (2009) Recording scapular motion using an acromion marker cluster. Gait Posture 29(1):123–128
29. van der Helm FCT (1994) A finite element musculoskeletal model of the shoulder mechanism. J Biomech 27(5):551–553, 555–569
30. van der Helm FCT, Pronk GM (1995) Three-dimensional recording and description of motions of the shoulder mechanism. J Biomech Eng 117(1):27–40
31. Veeger HEJ, van der Helm FCT (2007) Shoulder function: the perfect compromise between mobility and stability. J Biomech 40(10):2119–2129
32. Winby CR, Lloyd DG, Kirk TB (2008) Evaluation of different analytical methods for subject-specific scaling of musculotendon parameters. J Biomech 41(8):1682–1688
33. Wu G, van der Helm FCT, Veeger HEJ et al (2005) ISB recommendation on definitions of joint coordinate systems of various joints for the reporting of human joint motion–Part II: shoulder, elbow, wrist and hand. J Biomech 38(5):981–992
34. Zhou JL, Tits AL, Craig TL (1997) User's Guide for FFSQP Version 3.7: A FORTRAN code for solving constrained nonlinear (minimax) optimizaton problems, generating iterates, satisfying all inequality and linear constraints. University of Maryland